A Europium(III) Complex as an Efficient Singlet Oxygen Luminescence Probe

Bo Song,[†] Guilan Wang,[‡] Mingqian Tan,[†] and Jingli Yuan*,[†,‡]

Contribution from the Department of Analytical Chemistry, Dalian Institute of Chemical Physics, Chinese Academy of Sciences, Dalian 116023, P. R. China, and State Key Laboratory of Fine Chemicals, Department of Chemistry, Dalian University of Technology, Dalian 116012, P. R. China

Received April 29, 2006; E-mail: jingliyuan@yahoo.com.cn

Abstract: A new europium(III) complex, [4′-(10-methyl-9-anthryl)-2,2′:6′,2′′-terpyridine-6,6′′-diyl]bis(methylenenitrilo) tetrakis(acetate)$-Eu^{3+}$, was designed and synthesized as a highly sensitive and selective time-gated luminescence probe for singlet oxygen ($^1O_2$). The new probe is highly water soluble with a large stability constant of $\sim 10^{21}$ and a wide pH available range (pH 3$-$10), and can specifically react with $^1O_2$ to form its endoperoxide (EP-MTTA$-Eu^{3+}$) with a high reaction rate constant at 10^{10} M^{-1} s^{-1}, accompanied by the remarkable increases of luminescence quantum yield from 0.90% to 13.8% and lifetime from 0.80 to 1.29 ms, respectively. The wide applicability of the probe was demonstrated by detection of $^1O_2$ generated from a MoO_4^{2-}/H_2O_2 system, a photosensitization system of 5,10,15,20-tetrakis(1-methyl-4-pyridinio)-porphyrin tetra(*p*-toluenesulfonate) (TMPyP), and a horseradish peroxidase catalyzed aerobic oxidation system of indole-3-acetic acid (IAA). In addition, it was found that the new probe could be easily transferred into living HeLa cells by incubation with TMPyP. A time-gated luminescence imaging technique that can fully eliminate the short-lived background fluorescence from TMPyP and cell components has been successfully developed for monitoring the time-dependent generation of $^1O_2$ in living cells.

Introduction

The molecular oxygen of the lowest excited electronic state, singlet oxygen ($^1O_2$), has aroused much interest as a chemical and biological oxidant for environmental and biological systems. In the biological systems, it is thought to be an important toxic species in vivo since it can oxidize various kinds of biological molecules such as proteins, DNA, and lipids.[1−4] Singlet oxygen has also been proposed to be involved in the cell signaling cascade and in the induction of gene expression,[5,6] in changes in the mitochondrial membrane pore transition,[7] and is likely to play a key role in the bactericidal response of certain antibodies.[8] In another way, the artificial photochemical generation of $^1O_2$ has been used to destroy malignant cells or tissues as a cancer treatment protocol in a process called photodynamic therapy.[9−11]

Because of the outstanding importance of $^1O_2$ in photochemical and photobiological processes, several methods for $^1O_2$ detection have been established. Monitoring the direct emission of $^1O_2$ at 1270 nm is a specific and noninvasive method,[12−14] but this method suffers from weak signal because of the lower efficiency for $^1O_2$ emission, and quantitative detection of small amounts of $^1O_2$ is currently difficult in aqueous solution under physiological conditions, where the lifetime of $^1O_2$ is very short.[15] Furthermore, with this method it is difficult to measure the time-dependent formation amount of $^1O_2$. Absorbance-based probes, such as 2,5-dimethylfuran,[16] furfuryl alcohol,[17] 9,10-diphenylanthracene,[18] and *tert*-butyl-3,4,5-trimethylpyrrole-carboxylate,[19] rely on monitoring the loss of the probe molecules through reaction with $^1O_2$. Detection using these probes is still less sensitive because the method is based on the measurement of absorbance. Some sensitive fluorescent probes for $^1O_2$ have also been developed by incorporating the reactive anthracene

[†] Dalian Institute of Chemical Physics.
[‡] Dalian University of Technology.
(1) Epe, B.; Pflaum, M.; Boiteux, S. *Mutat. Res.* **1993**, *299,* 135−145.
(2) Kang, P.; Foote, C. S. *J. Am. Chem. Soc.* **2002**, *124*, 4865−4873.
(3) Davies, M. J. *Biochem. Biophys. Res. Commun.* **2003**, *305*, 761−770.
(4) Martinez, G. R.; Gasparutto, D.; Ravanat, J.-L.; Cadet, J.; Medeiros, M. H. G.; Mascio, P. D. *Free Radical Biol. Med.* **2005**, *38*, 1491−1500.
(5) Klotz, L. O.; Briviba, K.; Sies, H. *Methods Enzymol.* **2000**, *319*, 130−143.
(6) Ryter, S. W.; Tyrrell, R. M. *Free Radical Biol. Med.* **1998**, *24*, 1520−1534.
(7) Beghetto, C.; Renken, C.; Eriksson, O.; Jori, G.; Bernardi, P.; Ricchelli, F. *Eur. J. Biochem.* **2000**, *267*, 5585−5592.
(8) (a) Wentworth, P.; Jones, L. H.; Wentworth, A. D.; Zhu, X. Y.; Larsen; N. A.; Wilson, I.; Xu, X.; Goddard, W. A.; Janda, K. D.; Eschenmoser, A.; Lerner, R. A. *Science* **2001**, *293*, 1806−1811. (b) Wentworth, P.; McDunn, J. E.; Wentworth, A. D.; Takeuchi, C.; Nieva, J.; Jones, T.; Bautista, C.; Ruedi, J. M.; Gutierrez, A.; Janda, K. D.; Babior, B. M.; Eschenmoser, A.; Lerner, R. A. *Science* **2002**, *298*, 2195−2199.

(9) Weishaupt, K.; Gomer, C. J.; Dougherty, T. *Cancer Res.* **1976**, *36*, 2326−2329.
(10) Moan, J.; Berg, K. *Photochem. Photobiol.* **1992**, 55, 931−948.
(11) Henderson, B.; Dougherty, T. *Photochem. Photobiol.* **1992**, *55*, 145−157.
(12) Krasnovsky, A. A., Jr. *Biol. Membr.* **1998**, *15*, 530−548.
(13) Keszthelyi, T.; Weldon, D.; Andersen, T. N.; Poulsen, T. D.; Mikkelsen, K. V.; Ogilby, P. R. *Photochem. Photobiol.* **1999**, *70*, 531−539.
(14) Nonell, S.; Braslavsky, S. E. *Methods Enzymol.* **2000**, *319*, 37−49.
(15) Schweitzer, C.; Schmidt, R. *Chem. Rev.* **2003**, *103*, 1685−1757.
(16) Zepp, R. G.; Wolfe, N. L.; Baughman, G. L.; Hollis, R. C. *Nature (London)* **1977**, *267*, 421−423.
(17) Haag, W. R.; Hoigne, J. *Environ. Sci. Technol.* **1986**, *20*, 341−348.
(18) (a) Steinbeck, M. J.; Khan, A. U.; Karnovsky, M. J. *J. Biol. Chem.* **1992**, *267*, 13425−13438. (b) Steinbeck, M. J.; Khan, A. U.; Karnovsky, M. J. *J. Biol. Chem.* **1993**, *268*, 15649−15654.
(19) Denham, K.; Milofsky, R. E. *Anal. Chem.* **1998**, *70*, 4081−4085.

moiety into a xanthene ring.[20] These probes can react with $^1O_2$ to yield the corresponding endoperoxides giving sensitive fluorescence responses. There are a few limitations to these probes: they cannot be used at lower pH, where the endoperoxides are nonfluorescent, and they are obviously limited to steady-state investigations.[15] Recently, several sensitive chemiluminescence probes for $^1O_2$ based on a thiafulvalene substituted anthracene trap and dioxetane precursors have been reported.[21,22] However, the detection of $^1O_2$ in living cells using the above methods has rarely been studied.

Imaging is a useful tool for in vivo and in situ detection of $^1O_2$. The imaging of $^1O_2$ in living cells would provide a unique way to investigate the mechanisms of oxygen-dependent cell death. Microimaging of $^1O_2$ luminescence in cells has been reported recently,[23] but it required the use of D_2O to increase the luminescence lifetime of $^1O_2$, which is not applicable in vivo. Meanwhile, with imaging of the direct emission of $^1O_2$ at 1270 nm it is also difficult to measure the time-dependent accumulative amount of $^1O_2$ generated in the cells.

Time-gated fluorometry combined with the use of lanthanide complex-based luminescence probes (Eu^{3+} or Tb^{3+} complex) provides an excellent way for developing highly sensitive bioaffinity assays, in which short-lived background noise from both biological samples and the optical components can be effectively eliminated. Several reports have demonstrated that time-gated luminescence bioimaging microscopy technique is a powerful tool to eliminate fast decaying autofluorescence from biological specimens.[24−27] Therefore, this technique would be favored for the imaging detection of $^1O_2$ generation in living cells if only a lanthanide probe specific for $^1O_2$ and a suitable time-gated luminescence microscope were available.

Recently we have demonstrated that a Eu^{3+} complex, [4′-(9-anthryl)-2,2′:6′,2″-terpyridine-6,6″-diyl]bis(methylenenitrilo) tetrakis(acetate)−Eu^{3+} (ATTA−Eu^{3+}), and a Tb^{3+} complex, N,N,N^1,N^1-[2,6-bis(3′-aminomethyl-1′-pyrazolyl)-4-(9″-anthryl)-pyridine] tetrakis (acetate)−Tb^{3+} (PATA−Tb^{3+}), can be used as highly sensitive and selective time-gated luminescence probes for $^1O_2$.[28] Herein we report a further improved Eu^{3+} complex-based luminescence probe specific for $^1O_2$, [4′-(10-methyl-9-anthryl)-2,2′:6′,2″-terpyridine-6,6″-diyl]bis(methylenenitrilo) tetrakis(acetate)−Eu^{3+} (MTTA−Eu^{3+}), because the reaction rate of the 10-methyl-9-anthryl moiety in the new probe with $^1O_2$ is much faster than that of 9-anthryl moiety in ATTA−Eu^{3+} and

Scheme 1. Reaction of MTTA−Eu^{3+} with $^1O_2$
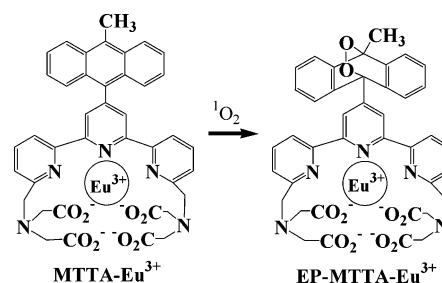
PATA−Tb^{3+},[29,30] which is more suitable for probing the short-lived $^1O_2$ in living cells. The new Eu^{3+} complex is almost nonluminescent, and can specifically react with $^1O_2$ to form highly luminescent endoperoxide (EP-MTTA−Eu^{3+}, Scheme 1) with a long luminescence lifetime, which makes the complex favorable for time-gated luminescence measurement. A strong luminescence response was found upon reaction of MTTA−Eu^{3+} with $^1O_2$ only, but not with other reactive oxygen species (ROS), such as hydroxyl radical, superoxide, hydrogen peroxide, and peroxynitrite, thus showing an extremely high specificity for $^1O_2$. To demonstrate the utility of the new probe for $^1O_2$ detection, the probe was applied for quantitative detection of $^1O_2$ generated from a MoO_4^{2-}/H_2O_2 system in a weakly basic buffer, the assay of $^1O_2$ formation by the irradiation of the photosensitizer 5,10,15,20-tetrakis(1-methyl-4-pyridinio)porphyrin tetra(*p*-toluenesulfonate) (TMPyP) in a neutral buffer, and the real-time monitoring of $^1O_2$ generation during the horseradish peroxidase (HRP)-catalyzed aerobic oxidation of indole-3-acetic acid (IAA) in a weakly acidic buffer. Furthermore, it was found that the new probe could be easily transferred into cultured HeLa cells by ordinary incubation together with TMPyP. A time-gated luminescence imaging technique that allows only the specific and long-lived luminescence signal to be imaged was successfully developed for monitoring the time-dependent generation of $^1O_2$ in the living Hela cells.

Results and Discussion

Probe Design and Characterization. In the previous works,[28] we have demonstrated that two lanthanide complexes, ATTA−Eu^{3+} and PATA−Tb^{3+}, can be used as highly sensitive and selective time-gated luminescence probes for $^1O_2$. To improve the probe's properties, especially its reaction rate with $^1O_2$, the 10-methyl-9-anthryl moiety in MTTA−Eu^{3+} was employed as a specific reactive moiety for trapping $^1O_2$ instead of the 9-anthryl moiety in ATTA−Eu^{3+} and PATA−Tb^{3+}, because the reaction rate constant of 10-methylanthracene with $^1O_2$ ($k = 9.6 \times 10^6$ M^{-1} s^{-1} in water)[29] is much higher than that of anthracene ($k = 1.6 \times 10^6$ M^{-1} s^{-1} in benzene, no data available in water).[30] The (2,2′:6′,2″-terpyridine-6,6″-diyl)bis(methylenenitrilo) tetrakis(acetate)−Eu^{3+} (TTA−Eu^{3+}) moiety was still chosen as a luminophore because of its higher luminescence quantum yield, stability, and solubility in aqueous buffers.[31]

The EP-MTTA−Eu^{3+}, synthesized by reacting MTTA−Eu^{3+} with chemically generated $^1O_2$ ($MoO_4^{2-}−H_2O_2$),[32] shows a high

(20) (a) Umezawa, N.; Tanaka, K.; Urano, Y.; Kikuchi, K.; Higuchi, T.; Nagano, T. *Angew. Chem., Int. Ed.* **1999**, *38*, 2899−2901. (b) Tanaka, K.; Miura, T.; Umezawa, N.; Urano, Y.; Kikuchi, K.; Higuchi, T.; Nagano, T. *J. Am. Chem. Soc.* **2001**, *123*, 2530−2536.

(21) Li, X. H.; Zhang, G. X.; Ma, H. M.; Zhang, D. Q.; Li, J.; Zhu, D. B. *J. Am. Chem. Soc.* **2004**, *126*, 11543−11548.

(22) (a) MacManus-Spencer, L. A.; Latch, D. E.; Kroncke, K. M.; McNeill, K. *Anal. Chem.* **2005**, *77*, 1200−1205. (b) MacManus-Spencer, L. A.; McNeill, K. *J. Am. Chem. Soc.* **2005**, *127*, 18954−18955.

(23) (a) Zebger, I.; Snyder, J. W.; Andersen, L. K.; Poulsen, L.; Gao, Z.; Lambert, J. D.; Kristiansen, U.; Ogilby, P. R. *Photochem. Photobiol.* **2004**, *79*, 319−322. (b) Snyder, J. W.; Skovsen, E.; Lambert, J. D. C.; Ogilby, P. R. *J. Am. Chem. Soc.* **2005**, *127*, 14558−14559.

(24) De Haas, R. R.; Verwoerd, N. P.; Van der Corput, M. P.; Van Gijlswijk, R. P.; Siitari, H.; Tanke, H. J. *J. Histochem. Cytochem.* **1996**, *44*, 1091−1099.

(25) Bjartell, A.; Laine, S.; Pettersson, K.; Nilsson, E.; Lövgren, T.; Lilja, H. *Histochem. J.* **1999**, *31*, 45−52.

(26) Connally, R.; Veal, D.; Piper, J. *Microsc. Res. Tech.* **2004**, *64*, 312−322.

(27) Weibel, N.; Charbonnière, L. J.; Guardigli, M.; Roda, A.; Ziessel, R. *J. Am. Chem. Soc.* **2004**, *126*, 4888−4896.

(28) (a) Song, B.; Wang, G.; Yuan, J. *Chem. Commun.* **2005**, 3553−3555. (b) Song, B.; Wang, G.; Tan, M.; Yuan, J. *New J. Chem.* **2005**, *29*, 1431−1438. (c) Tan, M.; Song, B.; Wang, G.; Yuan, J. *Free Radical Biol. Med.* **2006**, *40*, 1644−1653.

(29) Rubio, M. A.; Araya, L.; Abuin, E. B.; Lissi, E. A. *An. Asoc. Quim. Argent.* **1985**, *73*, 301−309.

(30) Stevens, B.; Perez, S. R.; Ors, J. A. *J. Am. Chem. Soc.* **1974**, *96*, 6846−6850.

(31) Latva, M.; Takallo, H.; Mukkala, V. M.; Matachescu, C.; Ubis, J. C. R.; Kankare, J. *J. Lumin.* **1997**, *75*, 149−169.

(32) Aubry, J. M.; Cazin, B. *Inorg. Chem.* **1988**, *27*, 2013−2014.

Table 1. Luminescence Properties of MTTA−Eu^{3+} and EP-MTTA−Eu^{3+} [a]

complex	$\lambda_{ex,max}$ (nm)	$\epsilon_{335\,nm}$ (cm^{-1}M^{-1})	$\lambda_{em,max}$ (nm)	ϕ (%)	τ (ms)
MTTA−Eu^{3+}	294, 335	18 100	614	0.90	0.80
EP-MTTA−Eu^{3+}	294, 335	16 400	614	13.8	1.29

[a] All data were obtained in 0.05 M borate buffer, pH 9.1.

stability in aqueous media. When EP-MTTA−Eu^{3+} was challenged with a 5-fold excess of ethylenediamine tetraacetic acid, a conditional stability constant was measured to be ∼10^{21} by Verhoeven's method.[33] No significant decrease of EP-MTTA−Eu^{3+} luminescence intensity was observed after several days at room temperature. Using the luminescence lifetimes of MTTA−Eu^{3+} and EP-MTTA−Eu^{3+} in H$_2$O and D$_2$O buffers, the average number (q) of water molecules in the first coordination sphere of Eu^{3+} ion was calculated from the equation[34] of $q = 1.2(1/\tau_{H_2O} - 1/\tau_{D_2O} - 0.25)$ to be 0.01 and 0.06, respectively. These results indicate that the new probe has high kinetic and thermodynamic stabilities, and the probe's increased luminescence intensity is not caused by a decrease in the number of the coordinated water molecules.[35]

The luminescence properties of MTTA−Eu^{3+} and EP-MTTA−Eu^{3+} are listed in Table 1. As expected, MTTA−Eu^{3+} itself is almost nonluminescent with a very low luminescence quantum yield (0.90%). Reacting with ^{1}O$_2$ to form EP-MTTA−Eu^{3+}, the Eu^{3+} complex becomes highly luminescent, with a 15.3-fold increase of the luminescence quantum yield and a 1.6-fold increase of the luminescence lifetime. Both MTTA−Eu^{3+} and EP-MTTA−Eu^{3+} have the typical Eu^{3+}-complex emission pattern (Figure 1A) with a main emission peak at 614 nm (^{5}D$_0$ → ^{7}F$_2$) and several side peaks centered at 585, 594, 647, and 692 nm, respectively. Similar to ATTA−Eu^{3+}, the two absorption bands between 360 and 410 nm caused by the absorption of 10-methyl-9-anthryl moiety in the probe disappeared after the formation of EP-MTTA−Eu^{3+} (Figure 1B), which indicates that it is a functional group acting to specifically trap ^{1}O$_2$ in the probe.[28]

The effects of pH on the luminescence intensity and lifetime of EP-MTTA−Eu^{3+} were measured by using a solution of 1.0 μM EP-MTTA−Eu^{3+} in 0.05 M Tris-HCl buffers with different pHs ranging from 1 to 10.2 (Figure 2). In contrast to the rapid decrease of fluorescence intensity of fluorescein-based probes at pH < 7,[20] the luminescence intensity of EP-MTTA−Eu^{3+} is stable at pH > 3 (the complex itself is not stable in a buffer of pH < 3). This result indicates that MTTA−Eu^{3+} is useful as a luminescence probe for ^{1}O$_2$ detection in weakly acidic, neutral, and basic buffers.

To investigate the reaction specificity of MTTA−Eu^{3+} with ^{1}O$_2$, the reactions of MTTA−Eu^{3+} with several ROS were examined in the same buffer. As shown in Figure 3, the luminescence intensities of the products of MTTA−Eu^{3+} reacted with ONOO$^-$, H$_2$O$_2$, •OH, and O$_2^{-•}$ did not change noticeably, whereas a remarkable increase was observed after the complex was reacted with ^{1}O$_2$. Since the luminescence intensities,

excitation, and emission spectra of the products of MTTA−Eu^{3+} reacted with ONOO$^-$, •OH, O$_2^{-•}$, and H$_2$O$_2$ are almost unchanged, we conclude that the complex does not react with these species. In addition, when enough azide, a quencher of ^{1}O$_2$,[36] was added to the ^{1}O$_2$−MTTA−Eu^{3+} system, luminescence enhancement of the complex was not observed. These results indicate that the luminescence probe MTTA−Eu^{3+} is highly specific for ^{1}O$_2$.

The reaction rate constants of ATTA−Eu^{3+} and MTTA−Eu^{3+} with ^{1}O$_2$ in a 0.05 M Tris-HCl buffer of pH 7.4 were determined by an established ESR method[37] using methylene blue as a photosensitizer[38] and 2,2,6,6-tetramethyl-4-piperidinol (TMP-OH) as a monitor of ^{1}O$_2$. TMP-OH was allowed to react with ^{1}O$_2$ to form a stable free radical, 2,2,6,6-tetramethyl-4-piperidinol oxide (TEMPO•), and then a typical three-line ESR spectrum of TEMPO• with equal intensities (a^N = 16.9 G, g = 2.0054) was recorded. Figure 4A shows the linear Stern−Volmer plot of the ESR signal intensity of TEMPO• against the concentration of ATTA−Eu^{3+} or MTTA−Eu^{3+}. The reaction rate constants of ATTA−Eu^{3+} and MTTA−Eu^{3+} with ^{1}O$_2$ were calculated to be 1.7×10^9 and 2.8×10^{10} M^{-1} s^{-1}, respectively. To confirm the results, a competitive experiment of the Eu^{3+} probe and sodium azide (NaN$_3$) with ^{1}O$_2$ was further employed to determine the reaction rate constant of the Eu^{3+} probe with ^{1}O$_2$. Figure 4B shows the linear Stern−Volmer plot of the luminescence intensity against the concentration of NaN$_3$. The reaction rate constants of ATTA−Eu^{3+} and MTTA−Eu^{3+} with ^{1}O$_2$ were calculated to be 3.3×10^9 and 6.0×10^{10} M^{-1} s^{-1}, respectively. The ^{1}O$_2$-associated of ATTA−Eu^{3+} and MTTA−Eu^{3+} reaction rate constants measured by the above two methods show good consistency, with average values of 2.5×10^9 M^{-1} s^{-1} for the ATTA−Eu^{3+}−^{1}O$_2$ reaction and 4.4×10^{10} M^{-1} s^{-1} for the MTTA−Eu^{3+}−^{1}O$_2$ reaction. However, they are obtained by indirect measurement methods and influenced by factors in the system, such as self-photosensitization, static quenching (when MTTA−Eu^{3+} was irradiated alone, its luminescence intensity had only a small increase, see Figure 7), and interactions of some solvent and buffer molecules with ^{1}O$_2$, so we may assume that the real reaction rate constants of ATTA−Eu^{3+} and MTTA−Eu^{3+} with ^{1}O$_2$ are at 10^9 and 10^{10} M^{-1} s^{-1}, respectively. Assuming that the detections of ATTA−Eu^{3+}−^{1}O$_2$ and MTTA−Eu^{3+}−^{1}O$_2$ reactions have the same experimental errors, we can conclude that the reaction of MTTA−Eu^{3+} with ^{1}O$_2$ is ∼17.5-fold faster than that of ATTA−Eu^{3+} with ^{1}O$_2$ in a neutral buffer, and MTTA−Eu^{3+} is more suitable to be used for probing the short-lived ^{1}O$_2$ in complex biological systems.

Compared to the rate constants for other (2 + 4) cycloaddition reactions of ^{1}O$_2$, the rate constants of the Eu^{3+} probes are much higher than those of other aromatic compounds.[39] Perhaps that is due to the influence of the conjugation of fluorophore (TTA−Eu^{3+} moiety) to the anthracene framework, since several reports

(33) Werts, M. H. V.; Verhoeven J. W.; Hofstraat, J. W. *J. Chem. Soc., Perkin Trans. 2* **2000**, 433−439.
(34) Beeby, A.; Clarkson, I. M.; Dickins, R. S.; Faulkner, S.; Parker, D.; Royle, L.; De Sousa, A. S.; Williams J. A. G.; Woods, M. *J. Chem. Soc., Perkin Trans. 2* **1999**, 493−504.
(35) Wolfbeis, O. S.; Dürkop, A.; Wu, M.; Lin, Z. H. *Angew. Chem., Int. Ed.* **2002**, *41*, 4495−4498.

(36) Harbour J. R.; Issler, S. L. *J. Am. Chem. Soc.* **1982**, *104*, 903−905.
(37) Weng, M.; Zhang, M.; Shen, T. *Dyes Pigm.* **1998**, *36*, 93−102.
(38) Turro, N. J.; Chow, M. F.; Rigaudy, J. *J. Am. Chem. Soc.* **1981**, *103*, 7218−7224.
(39) Lissi, E. A.; Encinas, M. V.; Lemp, E.; Rubio, M. A. *Chem. Rev.* **1993**, *93*, 699−723.
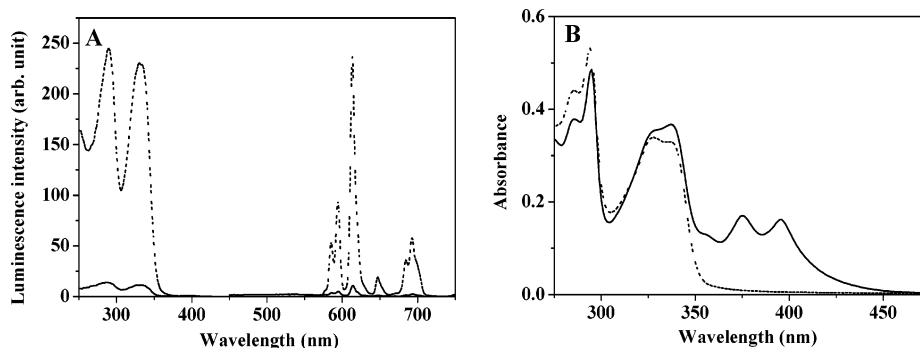
Figure 1. (A) Time-gated excitation and emission spectra of MTTA−Eu³⁺ (1.0 μM, solid line) and EP-MTTA−Eu³⁺ (1.0 μM, dashed line) in 0.05 M borate buffer of pH 9.1; (B) absorption spectra of MTTA−Eu³⁺ (20 μM, solid line) and EP-MTTA−Eu³⁺ (20 μM, dashed line) in 0.05 M borate buffer, pH 9.1.
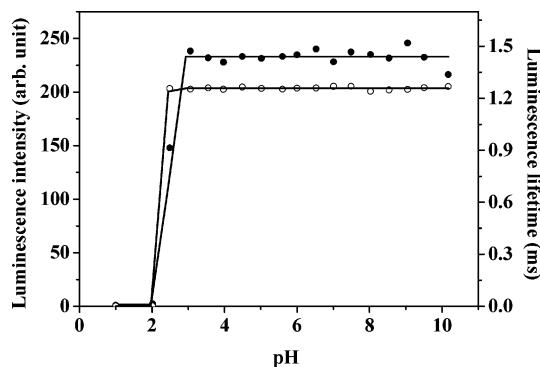

Figure 2. Effects of pH on the luminescence intensity (●) and lifetime (○) of EP-MTTA−Eu³⁺ (1.0 μM in 0.05 M Tris-HCl buffer).
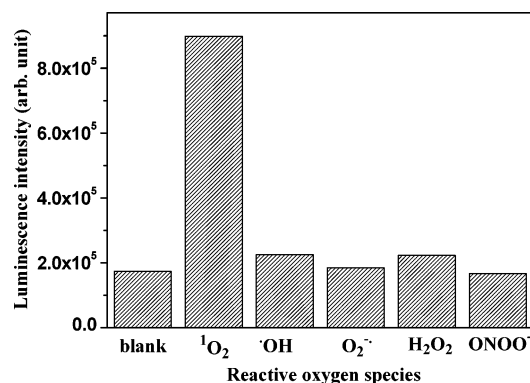

Figure 3. Luminescence intensities of the products of MTTA−Eu³⁺ (100 nM) reacted with different reactive oxygen species: $^1O_2$, 10 μM H_2O_2 + 10 mM Na_2MoO_4; •OH, 10 μM H_2O_2 + 10 μM ferrous ammonium sulfate; $O_2^{-•}$, 10 μM KO₂; H_2O_2, 10 μM H_2O_2.

have shown that lanthanide complexes are active catalysts for some (2 + 4) cycloaddition reactions as Lewis acid.[40]

Detection of $^1O_2$ Using MTTA−Eu³⁺ as a Probe in Aqueous Media. Because $^1O_2$ can be quantitatively generated in a weakly basic aqueous buffer through H_2O_2 disproportionation catalyzed by molybdate ions,[32] the $MoO_4^{2-}−H_2O_2$ system was used as a chemical source of $^1O_2$ to investigate the reaction of MTTA−Eu³⁺ with $^1O_2$. Figure 5 shows the time-gated excitation (5A) and emission (5B) spectra of MTTA−Eu³⁺ reacted with different concentrations of $^1O_2$ in 0.1 M carbonate

(40) (a) Yu, L. B.; Li, J.; Ramirez, J.; Chen, D. P.; Wang, P. G. *J. Org. Chem.* **1997**, *62*, 903−907. (b) Liao, S. J.; Yu, S. W.; Chen, Z, Y.; Yu, D. R.; Shi, L.; Yang, R. W.; Shen, Q. *J. Mol. Catal.* **1992**, *72*, 209−219. (c) Xu, X. P.; Ma, M. T.; Yao, Y. M.; Zhang, Y.; Shen, Q. *J. Mol. Struct.* **2005**, *743*, 163−168.

buffer of pH 10.5, which reveals the effect of the formation of EP-MTTA−Eu³⁺ on the luminescence intensity of the probe. The dose-dependent luminescence increase shows a good linearity between the luminescence intensity and the $^1O_2$ concentration with a wide concentration range of $^1O_2$ (Figure 6). The detection limit for $^1O_2$, calculated as the concentration corresponding to three standard deviations of the background signal, is 3.8 nM, which is ∼20-fold lower than that of the chemiluminescence method[21] and similar to that of ATTA−Eu³⁺ probe.[28]

Singlet oxygen produced by the irradiation of a photosensitizer in a neutral buffer was also detected by using MTTA−Eu³⁺ as a probe. A water-soluble cationic porphyrin, TMPyP, an efficient $^1O_2$ photosensitizer[41a] that has been studied in the context of photodynamic therapy,[41b] was used for this experiment. The luminescence intensity of the probe was monitored as a function of irradiation time. As shown in Figure 7, the luminescence intensity of the probe is distinctly increased with increase in irradiation time, which represents the production of $^1O_2$ during the irradiation, and provides reliable evidence for luminescence detection of $^1O_2$ using MTTA−Eu³⁺ as a probe.

The peroxidase-catalyzed oxidation of IAA plays an important role in IAA catabolism in vivo, which regulates plant growth at the molecular level.[42] Duran et al. and Kanofsky have previously proposed that $^1O_2$ is a product of the aerobic oxidation of IAA catalyzed by HRP at lower pH, but some results are still controversial.[43,44] In this work, the real-time monitoring of the kinetic process of $^1O_2$ generation in the aerobic oxidation of IAA catalyzed by HRP in a weakly acidic buffer was carried out using MTTA−Eu³⁺ as a probe under air. Figure 8A shows the reaction kinetic curves at different IAA concentrations. The luminescence intensity was increased over the reaction time until a steady value was reached when IAA was exhausted (because the experiments were carried out with an open system, the consumed O_2 of the reaction could be replenished from the air). In the investigated IAA concentration range, the increase rate of luminescence intensity (curve slope) paralleling the formation rate of EP-MTTA−Eu³⁺ is increased depending on the concentration of IAA. To measure the rate constant of EP-MTTA−Eu³⁺ formation in this reaction, we

(41) (a) Skovsen, E.; Snyder, J. W.; Lambert, J. D. C.; Ogilby, P. R. *J. Phys. Chem. B* **2005**, *109*, 8570−8573. (b) Villanueva, A.; Caggiari, L.; Jori, G.; Milanesi, C. *J. Photochem. Photobiol., B* **1994**, *23*, 49−56.
(42) Krylov, S. N.; Dunford, H. B. *J. Phys. Chem.* **1996**, *100*, 913−920.
(43) De Mello, M. P.; De Toledo, S. M.; Haun, M.; Cilento G.; Duran, N. *Biochemistry* **1980**, *19*, 5270−5275.
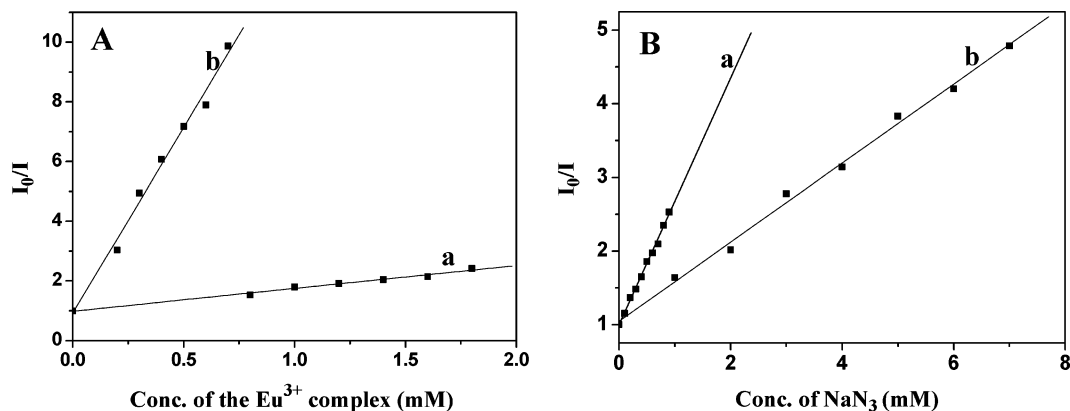(44) Kanofsky, J. R. *J. Biol. Chem.* **1988**, *263*, 14171−14175.

Figure 4. (A) Stern−Volmer plots of the ESR signal intensities of TEMPO• against the concentrations of ATTA−Eu³⁺ (a) and MTTA−Eu³⁺ (b); (B) Stern−Volmer plots of the luminescence intensities of the Eu³⁺ probes (a: ATTA−Eu³⁺, b: MTTA−Eu³⁺) against the concentrations of NaN₃.
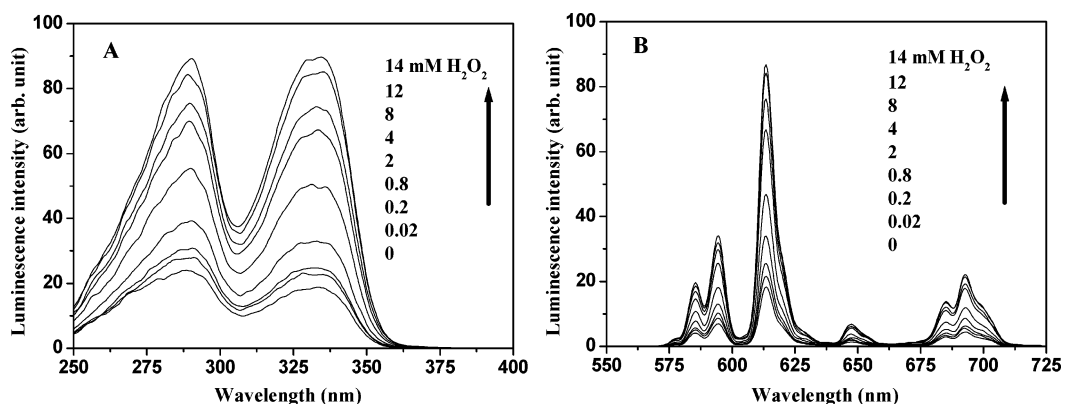

Figure 5. Time-gated excitation (A) and emission (B) spectra of MTTA−Eu³⁺ in the reaction with ¹O₂ generated from the MoO₄²⁻/H₂O₂ system.
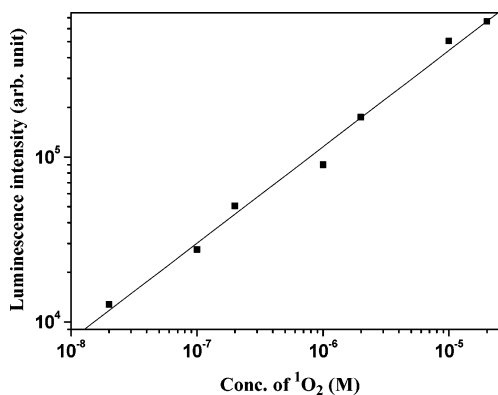

Figure 6. Calibration curve for ¹O₂ detection. The curve is derived from the luminescence intensity of the H₂O₂−MoO₄²⁻−MTTA−Eu³⁺ reaction in 0.1 M carbonate buffer of pH 10.5 with 100 nM of MTTA−Eu³⁺, 10 mM of Na₂MoO₄, and a series of standard H₂O₂ solutions.
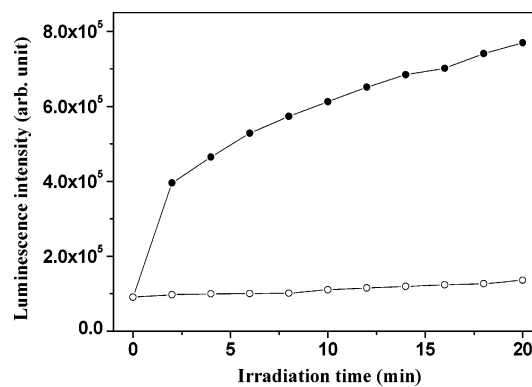

Figure 7. Reaction of MTTA−Eu³⁺ with ¹O₂ generated from photosensitization of TMPyP. Shown are 100 nM MTTA−Eu³⁺ + 100 nM TMPyP (●) and 100 nM MTTA−Eu³⁺ (○).

examined the correlation between IAA concentration and the initial rate of luminescence augmentation. Figure 8B depicts the dependence of the initial reaction rate on the concentration of IAA. A good linearity between the two parameters is obtained with a slope of 1.3×10^{-1}. Since the aerobic oxidation of IAA catalyzed by HRP is a very complex process and it is difficult to obtain the rate constant of the ¹O₂ generation from IAA-HRP system, only the total reaction rate constant (k_{tot}) of the IAA−HRP−MTTA−Eu³⁺ system [eq 1, where P = other products than EP-MTTA−Eu³⁺] was calculated (6.5×10^{10} M⁻¹ s⁻¹, from the relationship of reaction rate and concentrations of IAA and MTTA−Eu³⁺, which is 18-fold higher than that of the ATTA−Eu³⁺ probe).[28] This also indicates that the reaction

rate constant of MTTA−Eu³⁺ with ¹O₂ in an aqueous buffer is at the 10^{10} M⁻¹s⁻¹ level.

$$\text{MTTA−Eu}^{3+} + \text{IAA} \xrightarrow[\text{O}_2, \text{HRP}]{k_{tot}} \text{EP-MTTA−Eu}^{3+} + \text{P} \tag{1}$$
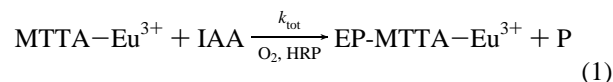
Time-Gated Luminescence Imaging of ¹O₂ Generation in Living Cells. The intent of the present work is to investigate the ¹O₂ generated by irradiation of a sensitizer deposited in living cells. To this end, TMPyP was incorporated into cultured Hela cells. The imaging result based on the 670 nm fluorescence of the TMPyP-deposited Hela cells (Figure 9) shows that TMPyP molecules mainly localize in the nucleus after transferring into the cells. However, a nonnegligible amount of TMPyP remains
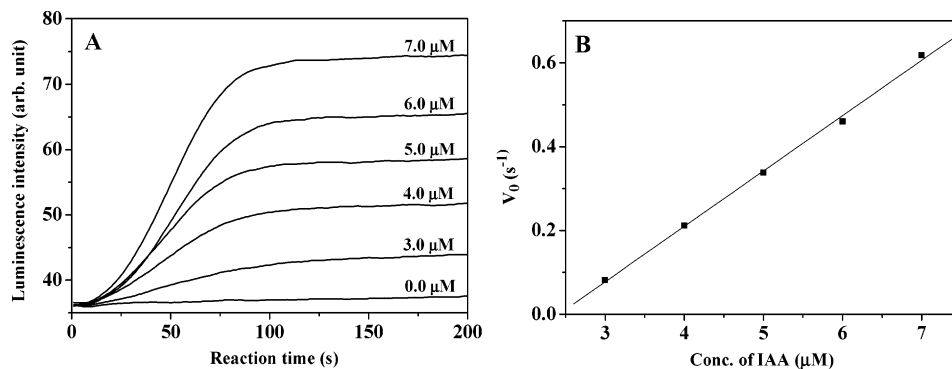
Figure 8. (A) Reaction kinetic curves of IAA−HRP−MTTA−Eu^{3+} system (2.0 μM MTTA−Eu^{3+} and 0.25 μM HRP) at different IAA concentrations. The measurements were carried out on a Perkin-Elmer LS 50B luminescence spectrometer with a time-gated luminescence mode and the following settings: delay time, 0.1 ms; gate time, 1.0 ms; cycle time, 20 ms; excitation wavelength, 335 nm; emission wavelength, 614 nm; excitation slit, 10 nm; emission slit, 5 nm; and data interval, 1.0 s. (B) The plot of initial rates (V_0) of the reaction of IAA−HRP−MTTA−Eu^{3+} against the IAA concentrations is shown.
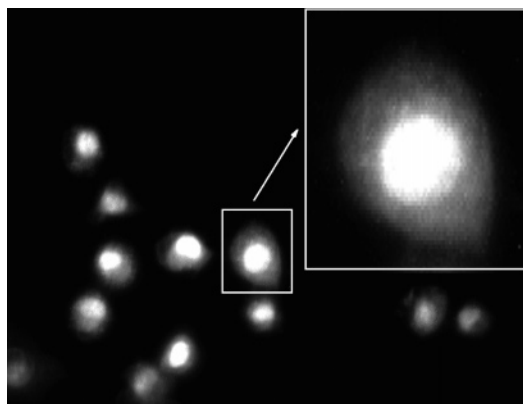

Figure 9. Fluorescence image of the TMPyP-deposited HeLa cells. The image was recorded by a CCD camera using a microscope-equipped 100 W mercury lamp as an excitation source (excitation filter, 450−490 nm; dichroic mirror, 505 nm; emission filter, > 520 nm).

Figure 10. Absorption spectra: (a) 10 μM TMPyP in distilled water; (b) 10 μM TMPyP + 50 μM MTTA−Eu^{3+} in distilled water; (c) the solution of curve b 5-fold diluted by distilled water.

in the cytoplasm. The ratio of nuclear to cytoplasmic TMPyP fluorescence is almost 3-fold.[41a,45a]

To investigate the time-dependent $^1O_2$ generation in the TMPyP-deposited Hela cells under irradiation, we tested several methods to prepare TMPyP−MTTA−Eu^{3+}-co-deposited Hela cells. When Hela cells were incubated with MTTA−Eu^{3+} followed by TMPyP, the time-gated luminescence intensities of the cells were not increased as function of irradiation time. In this case, only the TMPyP-deposited cells were obtained (Figure S5). This result suggests that MTTA−Eu^{3+} could not permeate through the cell membrane into the cells. However, it was found that MTTA−Eu^{3+} could be easily transferred into the living Hela cells by incubation together with TMPyP. A possible reason is that the Eu^{3+} probe can combine with TMPyP in the incubation solution to form a cation−anion pair [TMPyP]$^+$-[MTTA−Eu^{3+}]$^-$, and then be transferred into the cells by endocytosis just as endocytic vesicles carry TMPyP into the cells.[45] To confirm this hypothesis, we compared the UV−vis spectrum of TMPyP−MTTA−Eu^{3+} solution with the spectra of TMPyP and MTTA−Eu^{3+} and found that the absorption peak of TMPyP at 420 nm was shifted to 425 nm after it was mixed with MTTA−Eu^{3+}. When the solution was diluted, the peak at 425 nm was shifted back to 421 nm (Figure 10). These results suggest that the [TMPyP]$^+$[MTTA−Eu^{3+}]$^-$ pair could be
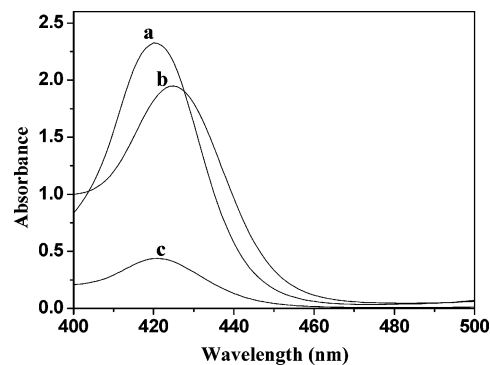
formed in concentrated solutions and dissociated upon dilution. This implies that our hypothesis should be reliable since the concentrations of TMPyP and MTTA−Eu^{3+} in the incubation solution of the cells are high enough (>10 μM) to form the TMPyP−MTTA−Eu^{3+} pair.

The TMPyP−MTTA−Eu^{3+}-deposited Hela cells were used for time-gated luminescence imaging to monitor intracellular $^1O_2$ generated by irradiation (the light of 450−490 nm) of a microscope-equipped 100 W mercury lamp on a time-gated luminescence microscope with an enough long delay time (400 μs) to fully eliminate luminescence emissions from TMPyP and the cell components. As shown in Figure 11, the luminescence intensities of four Hela cells are increased with irradiation time, indicating the increase of $^1O_2$ formed in the cells during the irradiation. It was observed that the luminescence enhancement of the cell nucleus (center of cell) is faster than that of the cytoplasm (fringe of cell) in a single cell. This result is caused by the fact that the TMPyP molecules principally localize in the nucleus and there more $^1O_2$ is produced.[23,41,42] Although the luminescence intensities of all cells are increased during the irradiation, the changes of the luminescence intensities of regions 1−4 (regions 1−3 are the center regions of three cells, and region 4 is an extracellular region) show that the $^1O_2$ productivities are different among the cells, and the $^1O_2$ productivities of three cells are increased in the order of cell 2 < cell 1 < cell 3 (Figure 12). This result demonstrates the fine spatial resolution of the luminescence imaging method. On the basis of the luminescence dilution curve of EP-MTTA−Eu^{3+} measured under the same conditions (Figure S6), the average

(45) (a) Georgiou, G. N.; Ahmet, M. T.; Houlton, A.; Silver, J.; Cherry, R. J. *Photochem. Photobiol.* **1994**, *59*, 419−422. (b) Snyder, J. W.; Lambert, J. D. C.; Ogilby, P. R. *Photochem. Photobiol.* **2006**, *82*, 177−184.
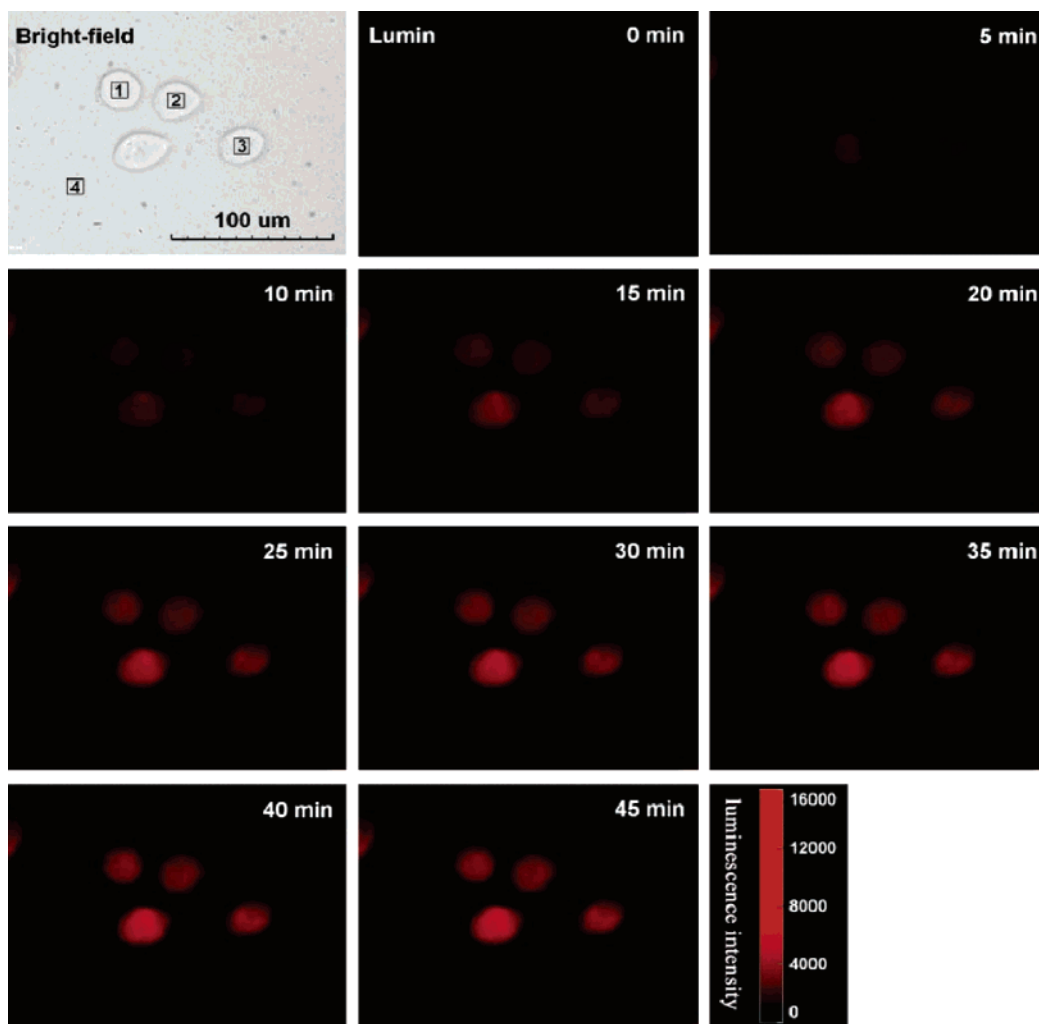
Figure 11. Bright-field (regions 1−3 are the center regions of three Hela cells, and region 4 is an extracellular region) and time-gated luminescence images of the TMPyP−MTTA−Eu^{3+}-deposited Hela cells at different irradiation times. The images are shown in pseudocolor (wavelength of 615 nm) corresponding to the luminescence intensity data in Figure 12.
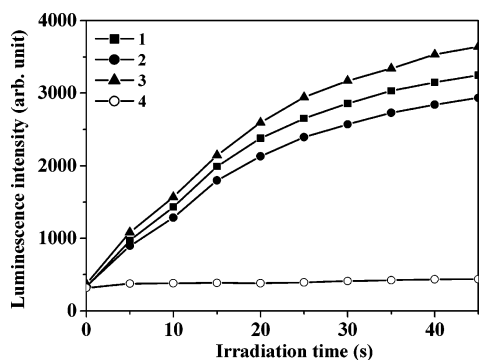

Figure 12. Luminescence intensities of the corresponding regions of Figure 11 at different irradiation times.

amount of the intracellular EP-MTTA−Eu^{3+} formed was estimated to be 18, 31, 37, and 41 μM after 10, 20, 30, and 40 min irradiation, respectively.

In contrast to the TMPyP−MTTA−Eu^{3+}-deposited cells, the time-gated luminescence imaging detection of the TMPyP-deposited cells did not show detectable responses before and after the cells were irradiated (Figure S5), this result indicates that the fluorescence of TMPyP does not interfere with the detection of the time-gated luminescence of MTTA−Eu^{3+}. During the irradiation of TMPyP−MTTA−Eu^{3+}-deposited cells,

the fluorescence intensity of TMPyP from the cells (principally localized in the nucleus) was decreased owing to photobleaching[45] (Figure S7). A recent report has shown that upon irradiation of a neuron freshly incubated with TMPyP, the fluorescence intensity of TMPyP initially increases because of a photoinduced release of TMPyP bound to DNA in the nucleus of the cell and then decreases because of photobleaching.[45b] In our experiments, the increase of fluorescence intensity of TMPyP was not observed. Furthermore, neither apoptosis nor necrosis of the TMPyP−MTTA−Eu^{3+}-deposited cells appeared to be induced during the irradiation. This could be due to the faster reaction of $^1O_2$ with MTTA−Eu^{3+} in the cells, which makes the reactions of $^1O_2$ with other cell components be inhibited (or reduced). It is also possible that the UV excitation light used for time-gated luminescence imaging (330−380 nm) is phototoxic to the cells. However, since a lower energy excitation source (30 W xenon flashlamp) and a shorter exposure time (60 s) were used for the time-gated luminescence imaging detections, UV-induced phototoxicity on the cells was not found.[46]

(46) Hanaoka, K.; Kikuchi, K.; Kojima, H.; Urano, Y.; Nagano, T. *J. Am. Chem. Soc.* **2004**, *126*, 12470−12476.

Conclusion

We have developed a Eu^{3+} complex-based luminescence probe specific for time-gated luminescence detection of $^1O_2$, MTTA–Eu^{3+}, by incorporating a luminophore of TTA–Eu^{3+} into 9-methylanthracene. The new probe can specifically and rapidly react with $^1O_2$ to form its endoperoxide, resulting in remarkable luminescence enhancement. Compared with previous reported $^1O_2$ probes, the advantages of this probe's high specificity, sensitivity, kinetic and thermodynamic stabilities, reaction rate constant, water solubility, and wide pH available range suggest that it should be widely useful for the time-gated luminescence detection of $^1O_2$ in many aqueous-based chemical and biological systems. The results shown here of time-gated luminescence imaging to monitor time-dependent $^1O_2$ generation in living cells demonstrate the utility of the probe for in vivo $^1O_2$ detection. The new technique, with fine time and spatial resolution capacities, provides a novel strategy for visualizing the temporal and spatial distribution of $^1O_2$ in cells and biological tissues, which would be a useful tool for cancer photodynamic therapy researches.[47,48]

Experimental Section

Reagents and Materials. The syntheses of [4′-(10-methyl-9-anthryl)]-2,2′:6′,2″-terpyridine-6,6″-diyl]bis(methylenenitrilo) tetrakis-(acetic acid) (MTTA) and EP-MTTA–Eu^{3+} were shown in Supporting Information. ATTA–Eu^{3+} was synthesized by using the previous method.[28] Horseradish peroxidase (RZ = 3.0, >250 U/mg) was purchased from Bio Basic Inc (Canada). Hela cells were obtained from Dalian Medical University. Anhydrous *N,N*-dimethylformamide (DMF), 2,2,6,6-tetramethyl-4-piperidinol (TMP–OH), and 10-methylanthracene-9-carboxaldehyde were purchased from Acros Organics (Belgium). 5,-10,15,20-Tetrakis(1-methyl-4-pyridinio)porphyrin tetra(*p*-toluenesulfonate) (TMPyP) was purchased from Fluka Chemistry (Switzerland). Tetrahydrofuran (THF) and acetonitrile were used after appropriate distillation and purification. Prior to use, hydrogen peroxide was diluted immediately from a stabilized 30% solution and was assayed by using its molar absorption coefficient of 43.6 $M^{-1}cm^{-1}$ at 240 nm.[49] Unless otherwise stated, all chemical materials were purchased from commercial sources and used without further purification.

Physical Measurements. The ^1H NMR spectra were recorded on a Bruker DRX 400 spectrometer (400 MHz). The MALDI-TOF-MS spectra were measured on a time-of-flight mass spectrometer (Biflex II, Bruker, Germany). Absorption spectra were measured on a Perkin-Elmer Lambda 35 UV–vis spectrometer. Elemental analysis was carried out on a Vanio-EL CHN analyzer. The ESR spectra were recorded at room temperature on a JES–FE1XG X-band spectrometer (JEOL, Tokyo, Japan) with 100 kHz field modulation and the following settings: central field, 3360 G; sweep width, 250 G; microwave power, 5 mV; response, 0.1 s. The time-gated luminescence spectra and luminescence properties (Figures 1A, 2, 5) were measured on a Perkin-Elmer LS 50B luminescence spectrometer with the following settings: excitation wavelength, 335 nm; emission wavelength, 614 nm; delay time, 0.2 ms; gate time, 1.0 ms; cycle time, 20 ms; excitation slit, 10 nm; and emission slit, 5 nm. The luminescence quantum yields (ϕ_1) of MTTA–Eu^{3+} and EP-MTTA–Eu^{3+} were measured in a 0.05 M borate buffer of pH 9.1 and calculated by using the equation $\phi_1 = I_1\epsilon_2C_2\phi_2/I_2\epsilon_1C_1$ with a standard luminescence quantum yield of $\phi_2 = 0.160$ for the Eu^{3+} complex with 4′-phenyl-2,2′:6′,2″-terpyridine-6,6″-diyl)bis-(methylenenitrilo) tetrakis(acetic acid) (molar extinction coefficient ϵ_{335}

nm = 14300 $cm^{-1}M^{-1}$).[31] In the equation, I_1 and I_2, ϵ_1 and ϵ_2, C_1 and C_2 are the luminescence intensities, molar extinction coefficients, and concentrations for the measured complex and the standard complex, respectively. The time-gated luminescence measurements (Figures 3, 4B, 6, 7) were carried out on a Perkin-Elmer Victor 1420 multilabel counter with an excitation wavelength of 340 nm, emission wavelength of 615 nm, delay time of 0.2 ms, window time (counting time) of 0.4 ms, and cycling time of 1.0 ms.

A fluorescence microscope that can be used for normal fluorescence imaging and time-gated fluorescence imaging was equipped by attaching a time-gated digital CCD camera system (Photonic Research Systems Ltd.), a cooled CCD camera (RET-2000R-F-CLR-12-C; Qimaging Ltd.), a 30 W xenon flashlamp (Pulse300, Photonic Research Systems Ltd.), a 100 W mercury lamp (C-LHG1, Nikon), a 40 × objective lens (CFI Plan Fluor ELWD DM 40 × C, Nikon), and epi-fluorescence filters (UV-2A, B-2A, G-2A; Nikon) on an inverted fluorescence microscope (TE2000-E; Nikon). The normal fluorescence imaging system was controlled by using an Imagex-TGi software (Photonic Research Systems Ltd.) or a SimplePCI software (Compix), and the time-gated fluorescence imaging system was controlled by Imagex-TGi software. The time-gated digital CCD camera system, xenon flashlamp, and UV-2A fluorescence filters (excitation filter, 330–380 nm; dichroic mirror, 400 nm; emission filter, > 420 nm) were used for the time-gated luminescence imaging measurements, and the cooled CCD camera, mercury lamp, and B-2A fluorescence filters (excitation filter, 450–490 nm; dichroic mirror, 505 nm; emission filter, > 520 nm) were used for normal fluorescence imaging measurements. The 100 W mercury lamp of the microscope was also used as a light source (the light of 450–490 nm was used) for photosensitizations of TMPyP-deposited Hela cells and TMPyP–MTTA–Eu^{3+}-deposited Hela cells. The time-gated luminescence imaging was carried out with the following measurement conditions: delay time, 400 μs; gate time, 1 ms; lamp pulse width, 5 μs; and exposure time, 60 s.

Reactions of MTTA–Eu^{3+} with Reactive Oxygen Species (ROS). All the reactions were carried out in 0.05 M carbonate buffer of pH 10.5 with the same MTTA–Eu^{3+} concentration (0.1 μM) for 4 h at room temperature. Peroxynitrite was synthesized from sodium nitrite (0.6 M) and H_2O_2 (0.65 M) in a quenched-flow reactor (excess H_2O_2 was used to minimize nitrite contamination). After the reaction, the solution was treated with MnO_2 to eliminate the excess H_2O_2. The concentration of the $ONOO^-$ stock solution was determined by measuring the absorbance at 302 nm with a molar extinction coefficient of 1670 $M^{-1}cm^{-1}$.[50] Superoxide solution was prepared by adding KO_2 to dry dimethyl sulfoxide and stirring vigorously for 10 min.[51] Hydroxyl radical ($\cdot$OH) was generated in the Fenton system from ferrous ammonium sulfate and hydrogen peroxide.[52] Singlet oxygen was chemically generated from the $MoO_4{}^{2-}$–H_2O_2 system in alkaline media.[32]

Detection of Reaction Rate Constant of the Eu^{3+} Probe with $^1O_2$. The reaction rate constants of the Eu^{3+} probes (MTTA–Eu^{3+} and ATTA–Eu^{3+}) with $^1O_2$ were determined by two independent methods. The detailed experimental procedures are as follows:

Method 1. The reaction rate constant of MTTA–Eu^{3+} or ATTA–Eu^{3+} with $^1O_2$ was determined by an electron spin resonance (ESR) spectroscopic method using the competitive reactions between the Eu^{3+} probe and TMP-OH with $^1O_2$ produced by the irradiation (a 100 W tungsten lamp was used) of methylene blue at room temperature in an oxygen-saturated solution. Different concentrations of the Eu^{3+} probe were used for the competitive reactions between the probe and TMP-OH (50 mM) with $^1O_2$ in 0.05 M Tris-HCl buffer of pH 7.4 containing

(47) Wilson, B. C.; Patterson, M. S.; Lilge, L. *Lasers Med. Sci.* **1997**, *12*, 182–199.
(48) Dougherty, T. J.; Gomer, C. J.; Henderson, B. W.; Jori, G.; Kessel, D.; Korbelik, M.; Moan, J.; Peng, Q. *J. Natl. Cancer Inst.* **1998**, *90*, 889–905.
(49) Lei, B.; Adachi, N.; Arai, T. *Brain Res. Protoc.* **1998**, *3*, 33–36.
(50) Miyamoto, S.; Martinez, G. R.; Martins, A. P. B.; Medeiros; M. H. G.; Mascio, P. D. *J. Am. Chem. Soc.* **2003**, *125*, 4510–4517.
(51) Zhao, H. T.; Kalivendi, S.; Zhang, H.; Joseph, J.; Nithipatikom, K.; Vasquez-Vivar, J.; Kalyanaraman, B. *Free Radical Biol. Med.* **2003**, *34*, 1359–1368.
(52) Setsukinai, K.; Urano, Y.; Kakinuma, K.; Majima, H. J.; Nagano, T. *J. Biol. Chem.* **2003**, *278*, 3170–3175.

0.1 mM methylene blue. In all the experiments, the solutions were irradiated outside the cavity in capillaries and the ESR spectra were recorded after 10 min exposure. A typical three-line ESR spectrum of TEMPO$^{\bullet}$ with equal intensities ($a^{N} = 16.9$ G, $g = 2.0054$) was recorded. The reaction rate constant of the Eu^{3+} probe with $^{1}O_2$ was calculated according to the eq 2,[37] where I_0/I is the ratio of the signal intensity of TEMPO$^{\bullet}$ radical in the absence and the presence of the Eu^{3+} probe, k_T is the rate constant for the TMP-OH$-^{1}O_2$ reaction[53] ($k_T = 4.0 \times 10^7$ M^{-1} s^{-1}), k_d is the decay rate of $^{1}O_2$ in an aqueous solution[54] ($k_d = 2.38 \times 10^7$ s^{-1}), k_q is the rate constant for the Eu^{3+} probe$-^{1}O_2$ reaction, [T] is the concentration of TMP-OH, and [Q] is the concentration of the Eu^{3+} probe.

$$\frac{I_0}{I} = 1 + \frac{k_q}{k_T[T] + k_d}[Q] \qquad (2)$$

Method 2. The reaction rate constant of MTTA$-$Eu^{3+} or ATTA$-$Eu^{3+} with $^{1}O_2$ was determined by a fluorometric method using the competitive reactions between the Eu^{3+} probe and sodium azide with $^{1}O_2$ produced by the irradiation of TMPyP at room temperature in an oxygen-saturated solution. Different concentrations of NaN$_3$ were used for the competitive reactions between the Eu^{3+} probe (10 μM) and NaN$_3$ with $^{1}O_2$ in 0.05 M Tris-HCl buffer of pH 7.4 containing 10 μM TMPyP. In the same way, the reaction rate constant of the Eu^{3+} probe with $^{1}O_2$ was calculated according to the eq 2, where I_0/I is the ratio of the luminescence intensity in the absence and the presence of NaN$_3$, k_T is the rate constant for the Eu^{3+} probe$-^{1}O_2$ reaction, k_d is the decay rate of $^{1}O_2$ in an aqueous solution[54] ($k_d = 2.38 \times 10^7$ s^{-1}), k_q is the rate constant for NaN$_3-^{1}O_2$ reaction[55] ($k_q = 4.5 \times 10^8$ M^{-1} s^{-1}), [T] is the concentration of the Eu^{3+} probe, and [Q] is the concentration of NaN$_3$.

Detection of $^{1}O_2$ in Aqueous Media. The reactions of MTTA$-$Eu^{3+} with $^{1}O_2$ generated from a MoO$_4^{2-}-$H$_2$O$_2$ system, a photosensitization system, and an HRP-catalyzed oxidation system of IAA were investigated. The detailed experimental procedures are described as follows:

(i) The reaction of MTTA$-$Eu^{3+} with $^{1}O_2$ generated from a MoO$_4^{2-}-$H$_2$O$_2$ system was performed in 0.1 M carbonate buffer of pH 10.5. Various concentrations of H$_2$O$_2$ solutions were added to the

buffer solutions containing 10 μM of MTTA$-$Eu^{3+} and 1 mM of Na$_2$MoO$_4$. After the reaction, the solutions were 10-fold diluted (final probe concentration $= 1.0$ μM) with 0.05 M borate buffer of pH 9.1, and the excitation and emission spectra were measured with a time-gated mode.

(ii) The photosensitization reaction was carried out in 0.05 M Tris-HCl buffer of pH 7.4. The buffer solution containing 10 μM TMPyP and 10 μM of MTTA$-$Eu^{3+} in a 1.0 cm quartz cell was irradiated from a distance of 2 cm by a 100 W tungsten lamp. After the reaction, the solution was 100-fold diluted (final probe concentration $= 100$ nM) with the buffer and subjected to the time-gated luminescence measurement.

(iii) The experiments of real-time monitoring of $^{1}O_2$ generation in an HRP-catalyzed oxidation system of IAA using the MTTA$-$Eu^{3+} as a probe were carried out in 0.05 M sodium acetate buffer of pH 4.0. To a series of IAA solutions (2.0 mL) containing 10 μM MTTA$-$Eu^{3+} were added 10 μL of 50 μM HRP (the molar concentration of HRP was calculated by using the molecular weight, M$_{HRP} = 40\ 000$) under constant stirring. The reaction kinetic curves were recorded simultaneously after the addition of HRP on a Perkin-Elmer LS 50B luminescence spectrometer with a time-gated mode.

Preparation of the Dye-Deposited Hela Cells. Hela cells were cultured in RPMI-1640 medium (Sigma-Aldrich, Inc.), supplemented with 10% fetal bovine serum (Corning Incorporated), 1% penicillin (Gibco), and 1% streptomycin (Gibco) at 37 °C in a 5% CO$_2$/95% air incubator. For detection of intracellular $^{1}O_2$, the cultured Hela cells in a 25 cm^2 glass culture bottle were washed three times with an isotonic saline solution consisting of 140 mM NaCl, 10 mM glucose, and 3.5 mM KCl, and then incubated with the isotonic saline solution containing 0.4 mM MTTA$-$Eu^{3+} and 10 μM TMPyP for 5 h at 37 °C in a 5% CO$_2$/95% air incubator.[23a] The cells were then washed five times with the isotonic saline solution and used for time-gated luminescence imaging measurement in the presence of the isotonic saline solution.

Supporting Information Available: The details of synthesis and characterization of MTTA, MTTA$-$Eu^{3+}, and EP-MTTA$-$Eu^{3+} and some results of control experiments for time-gated luminescence imaging. This material is available free of charge via the Internet at http://pubs.acs.org.

JA062990F

(53) Lion, Y.; Gandin, E.; Van de Vorst A. *Photochem. Photobiol.* **1980**, *31*, 305−309.
(54) Schmidt, R. *J. Am. Chem. Soc.* **1989**, *111*, 6983−6987.
(55) Miskoski, S.; Garcia, N. A. *Photochem. Photobiol.* **1993**, *57*, 447−452.